Molecular Crystals and Liquid Crystals

Publication details, including instructions for authors and subscription information:
http://www.tandfonline.com/loi/gmcl20

Liquid Crystal Nonlinear Optical Meta-Materials

I. C. Khoo [a], A. Diaz [a], J. Liou [a], D. Werner [a], J. H. Park [a], Y. Ma [a] & J. Huang [a]

[a] Department of Electrical Engineering, The Pennsylvania State University, University Park, PA, USA

Version of record first published: 01 Jun 2009

To cite this article: I. C. Khoo, A. Diaz, J. Liou, D. Werner, J. H. Park, Y. Ma & J. Huang (2009): Liquid Crystal Nonlinear Optical Meta-Materials, Molecular Crystals and Liquid Crystals, 502:1, 109-120

To link to this article: http://dx.doi.org/10.1080/15421400902815829

Mol. Cryst. Liq. Cryst., Vol. 502, pp. 109–120, 2009

ISSN: 1542-1406 print/1563-5287 online
DOI: 10.1080/15421400902815829

Taylor & Francis
Taylor & Francis Group

Liquid Crystal Nonlinear Optical Meta-Materials

I. C. Khoo, A. Diaz, J. Liou, D. Werner, J. H. Park, Y. Ma, and J. Huang
Department of Electrical Engineering, The Pennsylvania State University, University Park, PA, USA

We present an overview of metamaterials comprising nematic liquid crystals and nano-particulates or nano-structures. These metamaterials possess emergent properties such as electro-optically and all-optically tunable sub-unity, zero and negative refractive indices, and other properties not possible with conventional chemical synthesis methods. Optical wave mixing and self-action effects conducted with nano-particulate doped nematic liquid crystals have demonstrated fast optical field induced index modulation in micron- and sub-micron thin nematic films.

Keywords: enhanced birefringence; liquid crystals; metamaterials; nano-particulates; nano-structures; nonlinear optics; optical switching; sub-unity and negative index

1. INTRODUCTION

In both isotropic and ordered phases, liquid crystals possess extraordinarily large optical nonlinearities originating from a variety of individual and collective molecular processes. Among the ordered phases, nematic liquid crystals are perhaps the most widely studied ones as a result of their broadband birefringence and extreme sensitivity to perturbation by external fields. Optical nonlinearities such as laser induced refractive index change coefficients n_2 ranging from 10^{-4} to $10^3\,cm^2/W$ have been observed; almost all nonlinear optical processes have been demonstrated, including self-focusing, phase conjugation, stimulated scattering, solitons, photorefractivity, bistability

Plenary Paper presented at the *Liquid Crystal in Photonics Workshop*, Cambridge University, July 21, 2008. This work is supported by the Air Force Office of Scientific Research, the Army Research Office and the National Science Foundation Material Research Science and Engineering Center DMR-0820404.

Address correspondence to I. C. Khoo, Electrical Engineering Department, Pennsylvania State University, University Park, PA 16802, USA. E-mail: ick1@psu.edu

and instability, nonlinear optical processing ... etc [1–19]. Recent studies have centered on the use of nano-dopants and specialized structures to fashion new liquid crystalline metamaterials with emergent properties such as tunable sub-unity refractive indices ranging from positive through zero to the negative regimes, and photonic crystals in which light propagates in unconventional directions and velocities [20–26]. In comparison with other meta-material systems that tend to be passive and non-reconfigurable once they are fabricated, the presence of electro-optics and nonlinear optical materials such as liquid crystals enable tremendous tuning flexibility and new forms/shapes enabled by their dual (fluid/crystalline) physical properties.

In this paper, we present a quick review of two approaches to realizing liquid crystalline metamaterials and some recent preliminary experiments pointing to the feasibility of realizing these tunable materials in practice. The introduction of nano-dopants into the nematic bulk also enable new mechanisms leading to ultrafast optical switching possibilities and nonlinear optics in very thin films otherwise impossible in pure nematics.

2. LIQUID CRYSTALLINE NONLINEAR OPTICAL METAMATERIALS

As demonstrated in [25], the refractive index of a material n is defined by

$$n = \text{sign}\left(\cos\left(\frac{\theta_\varepsilon - \theta_\mu}{2}\right)\cos\left(\frac{\theta_\varepsilon + \theta_\mu}{2}\right)\right)\sqrt{\varepsilon_r\mu_r} = \text{sign}\left(\cos\theta_\varepsilon + \cos\theta_\mu\right)\sqrt{\varepsilon_r\mu_r} \tag{1a}$$

where it is understood the positive square root is to be taken and θ_ε and θ_μ are defined in the interval $(-\pi, \pi]$ by:

$$\varepsilon'_N + i\varepsilon''_N = \frac{\varepsilon'_r}{|\varepsilon_r|} + i\frac{\varepsilon''_r}{|\varepsilon_r|} \equiv \cos\theta_\varepsilon + i\sin\theta_\varepsilon \tag{1b}$$

$$\mu'_N + i\mu''_N = \frac{\mu'_r}{|\mu_r|} + i\frac{\mu''_r}{|\mu_r|} \equiv \cos\theta_\mu + i\sin\theta_\mu \tag{1c}$$

The sign of the refractive index is given by $\text{sign}(\cos\theta_\varepsilon + \cos\theta_\mu)$. Figures 1a–b show respectively the 3-D plots of the real and imaginary

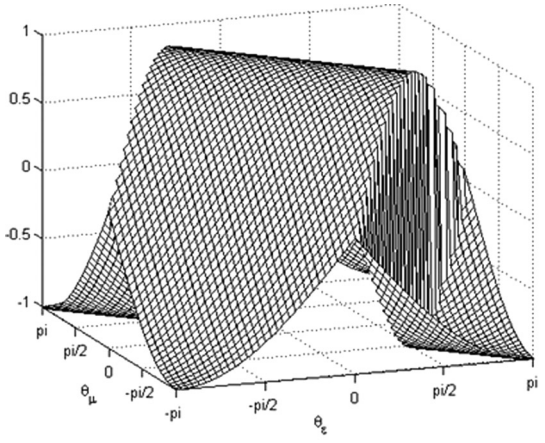

(a)

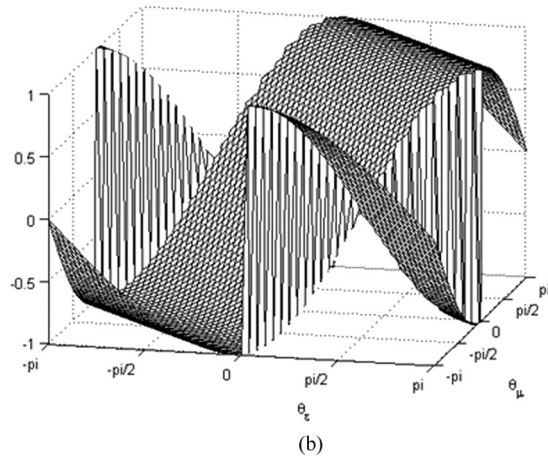

(b)

FIGURE 1 Plot of the (a) real part and (b) imaginary part of the normalized complex refractive index on the $\theta_\varepsilon - \theta_\mu$ phase space. Note that in the convention used, a positive (>0) imaginary part corresponds to loss.

part of the refractive index in the phase-space spanned by θ_ε and θ_μ. Clearly, for a particular value of the real part of the refractive index n, there are very many combination possibilities of θ_ε and θ_μ, corresponding to a wide ranging positive (loss) or negative (gain) values for the imaginary part of n. Also, there are vast regions in the $\theta_\varepsilon - \theta_\mu$ phase space where the real-part of refractive index can be zero or negative.

The central issue in the development of a metamaterial is the 'engineering' of the permittivity and permeability of the metamaterial

constituents in conjunction with specialized structures in order to access a desired value of the refractive index. We have pursued two promising approaches to realize these metamaterials: (A) Periodic metallo-dielectric nanostructures containing nematic liquids and (B) Random distribution of nano-particulates in bulk aligned liquid crystal cells.

2.1. Liquid Crystals in Periodic Metallo-Dielectric Nano-Structures

Metallo-dielectric planar periodic structures, often termed frequency selective surfaces [FSS] have been employed for very long wavelength (e.g. microwave and RF) electromagnetic applications for decades [21,22,26,27]. An example of such FSS-like metamaterial [21,22,26] structure is depicted in Figure 2. The unit cell consists of two aligned nematic liquid crystal layers sandwiching a metallo-dielectric nanostructure that is made up of a magnetic resonator (two strips of silver of thickness 30 nm separated by a thin layer of alumina of thickness 20 nm) surrounded by a negative permittivity material [thin silver films]. The space between neighboring magnetic resonators is filled with silica. A rigorous full-wave electromagnetic scattering analysis of the structure [21,22,26] showed that in some frequency interval,

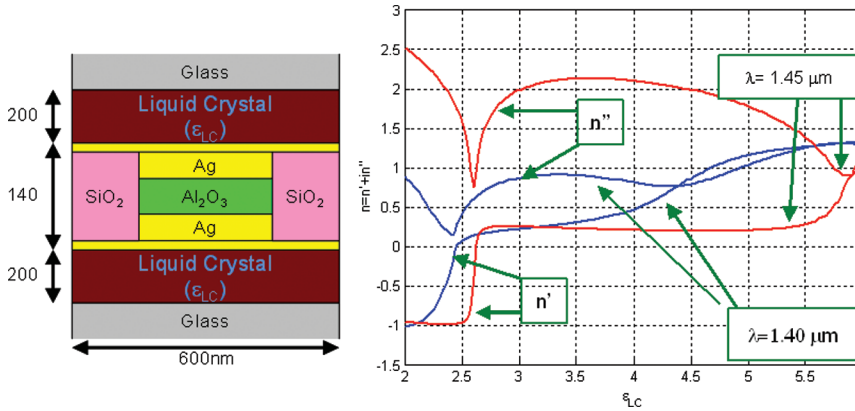

FIGURE 2 The 'unit cell' makeup of a periodic metallo-dielectric nanostructure containing magnetic resonator and negative permittivity material with tunable liquid crystal layers and exemplary results for the dependence of the complex refractive index on the liquid crystal dielectric constant for two optical wavelengths [after Ref. 22]. All dimensions are in nm. Note: Figure not drawn to scale in order to show details of the magnetic resonator.

the effective refractive index can assume unconventional values ranging from positive through zero and into the negative domain. Figure 2 shows the complex refractive index $n = n' + n''$ for two different incident light wavelengths as a function of the liquid crystal dielectric constant ε_{LC}. As a result of the tunable birefringence of the liquid crystal layers, the effective refractive index of this metamaterial can be varied over a wide range. For a typical nematic birefringence $\Delta n_{nlc} \sim 0.2$ ($n_e = 1.7$ and $n_o = 1.5$), the lower right solid curve for incident light wavelength $\lambda = 1.45\,\mu m$ shows that the effective index can be varied from -1 to 0.3, i.e. an effective refractive index change Δn_{eff} of 1.3. Such enhanced birefringence obviously will lead to enhanced optical nonlinearities as well as electro-optics responses [18].

The major problems confronting these approaches stem from the precise nanometer-scale fabrication requirements, and large absorption losses associated with the metals or 'plasmonic' material constituents. Also, the strong anchoring of the liquid crystal molecules in such highly confined geometries would require prohibitively large electric fields. As demonstrated in section 3, nonlinear all-optical means provide an 'electrode-less' and more flexible means of creating index changes and the desired optical properties/functions. Moreover, as a result of the extraordinarily large optical nonlinearity of nematics, these index changes can be induced at low power and high speed.

2.2. Nano-Particulate Suspensions in Bulk Liquid Crystals

An alternative approach to realizing tunable index materials is to employ well established bottom-up methods for synthesizing monodispersed spheres, core-shell nanostructures, and nanorods that contain plasmonic metals or other appropriate dielectric components,

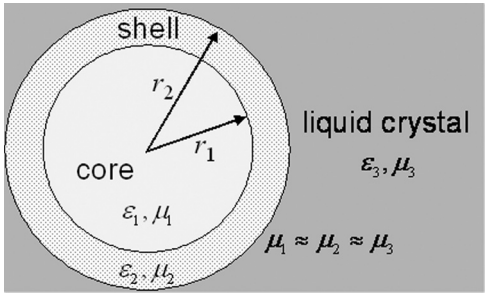

FIGURE 3 Schematic of core-shell nano-spheres dispersed in aligned nematic liquid crystal layer.

and disperse them in a host medium. Figure 3 shows a schematic of an aligned nematic liquid crystal doped with randomly dispersed core-shell nano-spheres. The liquid crystal host provides the tunable permittivity, while the nano-particulates provide the desired permittivity and permeability to create the desired effective refractive indices. The complex effective refractive index of such metamaterial is calculated through the Clausius-Mosotti relations from Mie scattering coefficients a_1 and b_1 (these are the dipole terms of the scattered magnetic fields), according to the expressions [28–30]:

$$\varepsilon_r^{eff} = \varepsilon_{host}\left(\frac{k_{host}^3 + i4\pi N a_1}{k_{host}^3 - i2\pi N a_1}\right) \tag{2a}$$

$$\mu_r^{eff} = \frac{k_{host}^3 + i4\pi N b_1}{k_{host}^3 - i2\pi N b_1} \tag{2b}$$

where k_{host} is the optical wave vector in the host fluid, $\varepsilon_{\text{host}}$ is the permittivity of the host, and N is the volume density of the nanospheres.

We have studied several cases involving gold and silver nanospheres and gold- or silver- coated silica spheres of diameter in the order of a few nm's. A Lorentz-Drude model [31] is used to describe the complex dielectric functions of gold and silver. In such nanoparticles (diameter $<$10 nm), the small dimension limits the mean free path of free electrons resulting in increased surface scattering. This effect can be modeled by adding a surface scattering rate $\omega_S = Av_f/r$ to the damping constant γ_0 in the free-electron Drude model [32–35], resulting in:

$$\varepsilon(\omega, r) = \varepsilon_{bulk}(\omega) + \frac{\omega_p^2}{\omega^2 + i\omega\gamma_0} - \frac{\omega_p^2}{\omega^2 + i\omega(\gamma_0 + Av_F/r)} \tag{3}$$

This model has been shown to be effective in describing the optical characteristics of gold- and silver-dispersed nanoparticles at different concentrations when compared to previously reported measurements using spectroscopic ellipsometry in the visible and near-infrared region [36].

The optical permittivity of the host nematic liquid crystal (NLC) for a linearly polarized light incident at an oblique angle θ is given by [18]

$$\varepsilon_{host} = \frac{\varepsilon_e \varepsilon_o}{\varepsilon_e \cos^2\theta + \varepsilon_o \sin^2\theta} \tag{4}$$

where ε_e and ε_o are the respective permittivities for light polarized parallel and perpendicular to the director axis $\hat{n}$ and θ is the angle made by the director axis with the optical wave vector k_0. Note that $\varepsilon_{\text{host}}$ does not carry any resonant dependence except for some small variation over the optical- infrared wavelength regime of interest here.

We have studied a variety of nano-spheres [solid or core-shell] in various combinations and liquid crystal alignments. Some exemplary results for the effective refractive indices are shown in Figures 4 and 5, calculated using various plasmonic frequencies, damping constants . . . etc for Au and Ag [28,31]. Figures 4a–b shows respectively, the calculated real (n) and imaginary (k) part of refractive index for 2 nm radius gold and silver nano-particles while Figures 5a–b show the results for the case of Au- or Ag-coated silica spheres [the radius for the silica core is 10 nm with a permittivity of 3.8, and the thickness

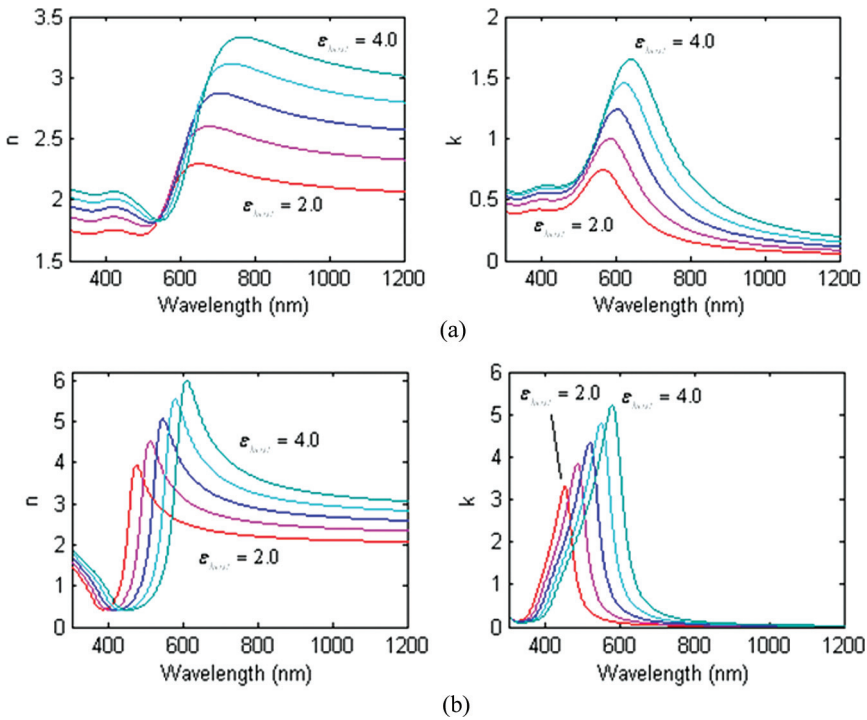

FIGURE 4 Calculated real (n) and imaginary (k) part of the effective refractive index of liquid crystal with nano-particles dispersion as the permittivity of the liquid crystal is varied from 2.0 to 4.0 in steps of 0.5. (a) 2 nm solid gold nano-spheres (b) 2 nm solid silver nano-spheres.

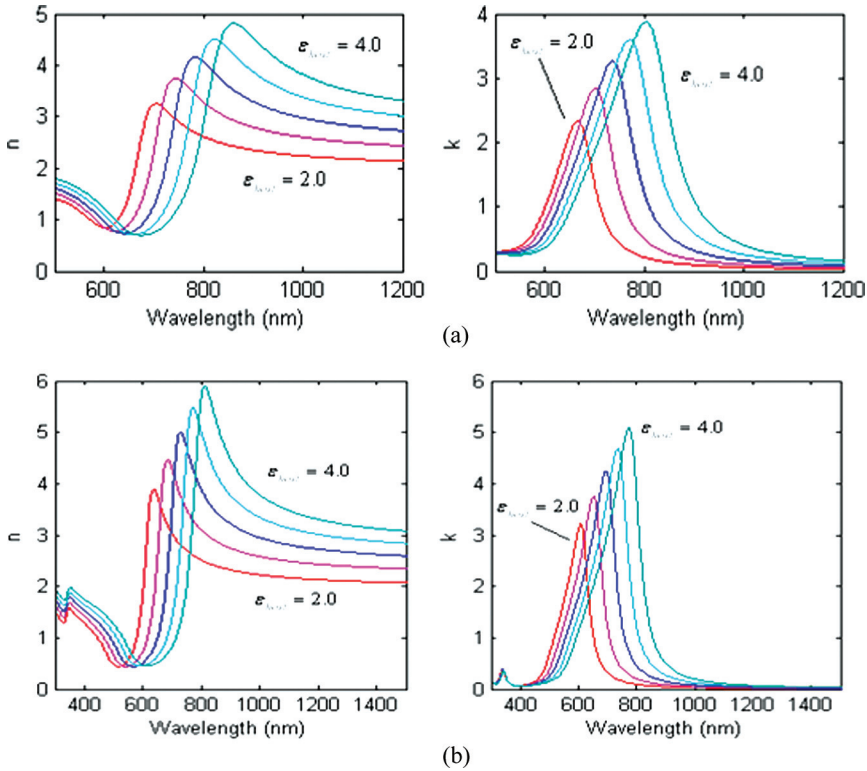

FIGURE 5 Calculated real (n) and imaginary (k) part of the effective refractive index of liquid crystal with core-shell nano-particles dispersion as the permittivity of the liquid crystal is varied from 2.0 to 4.0 in steps of 0.5 for (a) 5 nm thick gold shell and (b) 5 nm thick silver shell. The silica core radius is 10 nm.

for the shell (gold or silver) is 5 nm]. The filling fraction is 0.25. The permittivity of the host medium (NLC) is varied from 2.0 to 4.0 in step of 0.5.

It is interesting to note that, besides enhanced birefringence, in some cases [Ag nano-spheres in Fig. 4b and Au- and Ag- core-shell nano-spheres in Figs. 5a–b], the effective refractive index of the LC metamaterial can be unity (1) or sub-unity (<1), a region not possible to access with conventional chemical synthesis methods. Some of these theoretical results have been shown to agree very well with experimental measurements of Au- nanospheres dispersed in polymer matrix [36]. Work is underway in dispersing Au- and Ag-nanospheres in nematic liquid crystals.

3. NONLINEAR OPTICAL RESPONSES OF VERY THIN NEMATIC LAYER

The tunability of the optical properties of these metamaterials is hinged on the electro-optical and nonlinear optical response of the birefringent nematic liquid crystal constituent. In the case of metallo-dielectric nanostructures discussed in section 2.1, the sub-micron thin nematic layer would require a prohibitively enormous electric field for electro-optical modulation, since the molecules adjacent to the boundary surfaces are strongly anchored. On the other hand, optical field induced thermal and order parameter changes in dye doped nematic offer a viable mechanism for creating the required refractive index [dielectric permittivity] changes in the NLC. This was indeed demonstrated in a recent optical wave-mixing experiment involving very thin nematic liquid crystal films ranging from 250 nm to ~1 micron.

Figure 6 shows an optical wave-mixing experimental set up used. A linearly polarized CW 532 nm laser is divided into two coherent beams which are then overlapped onto a nematic liquid crystal cell at a small crossing angle of about 0.01radian. The beam diameter on the sample is ~5 mm. The homeotropically aligned liquid crystal cells are made with methyl-red doped 5CB (Pentyl-Cyano-Biphenyl) with thicknesses ranging from ~250 nm to 1.7 μm as measured by Fabry-Perot interferometry before the cell is filled. The methyl-red dye concentration used is 2.5% by weight which is needed to yield visible self-diffraction from such thin samples under milliwatts laser power. Visible self-diffraction from these thin nematic films are manifested at an input laser power of 50mW (intensity of $\sim 200\,\mathrm{mW/cm^2}$). In Table 1 we list some of the typical results obtained. Note that in general, the optical nonlinearity n_2 [defined by index change $\Delta n = n_2 I$,

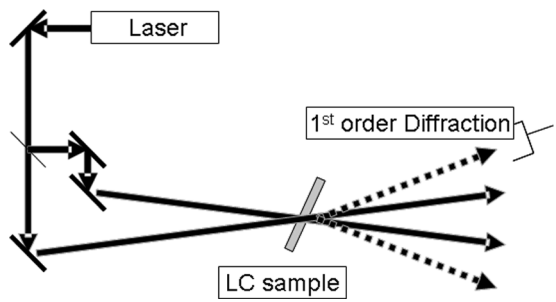

FIGURE 6 Schematic of the optical wave mixing experiment set up to measure self-diffraction efficiency from aligned nematic liquid crystal cells.

TABLE 1 Experimental Observed Self-Diffraction Efficiency and Nonlinear Index Coefficients of Very Thin Aligned Nematic Liquid Crystal Layer

Thickness (μm)	Input beam power (mW)	1st. order diffracted beam power (μW)	Diffraction efficiency	Nonlinear coefficient n_2 (cm^2/w)
0.25	50	25	5×10^{-4}	7.5×10^{-2}
0.8	54	33	6.11×10^{-4}	2.4×10^{-2}
1.2	50	850	170×10^{-4}	9×10^{-2}
1.7	38	245	64.5×10^{-4}	5.3×10^{-2}

where I is the optical intensity] of these samples are quite large, ranging from $2 \times 10^{-2} - 9 \times 10^{-2}\,cm^2/W$.

For linearly polarized input lasers incident on the sample in the normal direction, the index changing mechanism is due to optically induced thermal effect and order parameter change. The maximum refractive index change possible from this mechanism is on the order of $(n_{iso} - n_o) \sim (1.62 - 1.52) \sim 0.1$ using 5CB. It is noteworthy that a nematic layer as thin as 250 nm exhibits a significant optically induced index modulation Δn on the order of 0.015 with an input optical intensity of $0.2\,W/cm^2$ in the un-optimized geometry/sample. With optimization by using larger birefringence nematics and initial director axis alignment and laser polarization direction, much higher index modulation could be achieved.

These preliminary studies have demonstrated the feasibility of all-optical index modulation of nanostructures containing very thin layers of nematic liquid crystal. In contrast to previous studies of ac field induced index tuning in photonic crystals, however, all-optical tuning in this case is electrode-free and the applied field direction can be quite flexible. Furthermore, optical field induced index modulation is a much faster process. As demonstrated in a recent study, the response time can be as short as 50 μs in a 20 μm thick cell with CW laser [37,38]; sub-microsecond and nanosecond response times can be expected with short pulsed lasers [3,10,18]. Work is currently underway in realizing such ultrafast (for nematics) all-optical switching processes.

REFERENCES

[1] Khoo, I. C., Slussarenko, S., Guenther, B. D., & Wood, W. V. (1998). *Opt. Letts.*, *23*, 253–255.

[2] Lucchetti, L., Di Fabrizio, M., Francescangeli, O., & Simoni, F. (2004). *Opt. Comm.*, *233*, 417.

[3] Khoo, I. C., Lindquist, R. G., Micahel, R. R., & Mansfield, R., et al. (1991). *J. Appl. Phys.*, *69*, 3853–3859.
[4] Peccianti, M., Derossi, A., Assanto, G., de Luca, A., Umeton, C., & Khoo, I. C. (2000). *Appl. Phys. Lett.*, *77*, 7.
[5] Carbone, V., Cipparrone, G., Versace, C., Umeton, C., & Bartolino, R. (1996). *Phys. Rev.*, *E54*, 6948–6951.
[6] Khoo, I. C. & Diaz, A. (2003). *Phys. Rev.*, *E68*, 042701-1 to-4.
[7] Khoo, I. C. & Ding, J. (2002). *Appl. Phys. Letts.*, *81*, 2496–2498.
[8] Khoo, I. C. & Liang, Y. (2000). *Phys. Rev.*, *E62*, 6722–6733.
[9] Khoo, I. C., Li, H., & Liang, Yu. (1993). *Opt. Lett.*, *18*, 3.
[10] Khoo, I. C. & Normandin, R. (1984). *Optics Letts.*, *9*, 285–287.
[11] Khoo, I. C., Diaz, A., Kubo, S., Liou, J., Stinger, Mike Mallouk, T., & Park, J. H. (2008). *Molecular Crystals Liquid Crystals, 485:1*, 934–944.
[12] Khoo, I. C. & Shepard, S. (1983). *J. Appl. Phys.*, *54*, 5491–5493.
[13] Khoo, I. C., Ding, J., & Zhang, Y., et al. (2003). *Appl. Phys. Letts.*, *82*, 3587–3589.
[14] Khoo, I. C., Shih, Min-Yi., Wood, M. V., Guenther, B. D., Chen, P. H., Simoni, F., Slussarenko, S., Francescangeli, O., & Lucchetti, L. (1999). IEEE proceedings special issue on photorefractive optics: Materials, devices and applications. *IEEE Proceedings*, *87*(11), 1897–1911.
[15] Khoo, I. C., Wood, M. V., Shih, M. Y., & Chen, P. H. (1999). *Optics Express*, *4*(11), 431–442.
[16] Kaczmarek, M., Dyadyusha, A., Slussarenko, S., Khoo, I. C., et al. (2004). *J. Appl. Phys.*, *96*, 2616–2623.
[17] Shih, M. Y., Shishido, A., & Khoo, I. C. (2001). *Opt. Letts.*, *26*, 1140–1142.
[18] Khoo, I. C. (2007). *Liquid Crystals*, 2nd ed., Wiley: NJ.
[19] Khoo, I. C., Werner, D. H., Kwon, D. H., & Diaz, A. (2008). *Mole. Cryst. Liq. Cryst.*, *488*, 488–499.
[20] Khoo, I. C., Werner, D. H., Liang, X., Diaz, A., & Weiner, B. (2006). *Optics Letts.*, *31*, 2592.
[21] Wang, X., Kwon, D. H., Werner, D. H., Khoo, I. C., Kildishev, A., & Shalaev, V. M. (2007). *Appl. Phys. Lett.*, *91*, 143122.
[22] Werner, H., Kwon, D.-H., Khoo, I. C., Kildeshev, A. K., & Shalaev, V. M. (2007). *Optics Express*, *15*(6), 3342–3347.
[23] Graugnard, E., King, J. S., Jain, S., Summers, C. J., Zhang-Williams, Y., & Khoo, I. C. (2005). *Phys. Rev.*, *B72*, 233105.
[24] Khoo, I. C., Williams, Yana., Diaz, Andres., Chen, Kan., Bossard, J., Werner, D., Graugnard, E., & Summers, C. J. (2006). *Molecular Crystal Liquid Crystal*, *453*, 309–319.
[25] Diaz, A., Park, J. H., & Khoo, I. C. (2007). *JNOPM*, *16*, 533–549.
[26] Bossard, J. A., Liang, X., Li, L., Werner, D. H., Weiner, B., Cristman, P. F., Diaz, A., & Khoo, I. C. (2008). *IEEE Transactions on Antennas and Propagation*, *56*, 1308–1320.
[27] Wu, FSS T. K. (1995). *Frequency Selective Surface and Grid Array*. Wiley: New York.
[28] Doyle, W. T. (1989). *Phy. Rev. B*, *39*(14), 9852–9858.
[29] Jackson, J. D. (1999). *Classical Electrodynamics,* 3rd ed., Wiley: New York.
[30] Bohren, C. F. & Huffman, D. R. (1983). *Absorption and scattering of light by small particles*, Wiley: New York, pp. xiv, 530.
[31] Rakic, A. D., Djurisic, A. B., Elazar, J. M., & Majewski, M. L. (1998). *Applied Optics*, *37*(22), 5271–5283.

[32] Hövel, H., Fritz, S., Hilger, A., Kreibig, U., & Vollmer, M. (1993). *Physical Review B*, *48*(24), 18178–18188.
[33] Palpant, B., Prevel, B., Lerme, J., Cottancin, E., Pellarin, M., Treilleux, M., Perez, A., Vialle, J. L., & Broyer, M. (1998). *Physical Review B*, *57*(3), 1963–1970.
[34] Alvarez, M. M., Khoury, J. T., Schaaff, T. G., Shafigullin, M. N., Vezmar, I., & Whetten, R. L. (1997). *J. Phys. Chem. B*, *101*(19), 3706–3712.
[35] Kreibig, U. (1970). *Zeitschrift Fur Physik*, *234*(4), 307.
[36] Kubo, S., Diaz, A., Tang, Y., Mayer, T. S., Khoo, I. C., & Mallouk, T. E. (2007). *Nano Letters*, *7*(11), 3418–3423.
[37] Khoo, I. C., Park, J.-H., & Liou, J. D. (2007). *Appl. Phys. Letts.*, *90*, 151107.
[38] Khoo, I. C., Park, J.-H., & Liou, J. D. (2008). *J. Opt. Soc. Am. B*, (In Press).